Determination of the percolation threshold in Fe/MgO magnetic granular multilayers

2010 J. Phys.: Condens. Matter 22 056003

(http://iopscience.iop.org/0953-8984/22/5/056003)

J. Phys.: Condens. Matter **22** (2010) 056003 (8pp) doi:10.1088/0953-8984/22/5/056003

Determination of the percolation threshold in Fe/MgO magnetic granular multilayers

A García-García[1,2], A Vovk[3,4], P Štrichovanec[3], J A Pardo[3,5], C Magén[3], P A Algarabel[1,2], J M De Teresa[1,2], L Morellón[1,2,3] and M R Ibarra[1,2,3]

[1] Instituto de Ciencia de Materiales de Aragón, Universidad de Zaragoza-CSIC, 50009-Zaragoza, Spain
[2] Departamento de Física de la Materia Condensada, Universidad de Zaragoza, 50009-Zaragoza, Spain
[3] Instituto de Nanociencia de Aragón, Universidad de Zaragoza, 50018-Zaragoza, Spain
[4] Institute of Magnetism NAS of Ukraine, 36-b Vernnadsky boulevard, 03142, Kyiv, Ukraine
[5] Departamento de Ciencia y Tecnología de Materiales y Fluidos, Universidad de Zaragoza, 50018-Zaragoza, Spain

E-mail: vovk@imag.kiev.ua

Received 4 September 2009, in final form 17 December 2009
Published 15 January 2010
Online at stacks.iop.org/JPhysCM/22/056003

Abstract
The evolution of the morphology, magnetic and transport properties of Fe(t nm)/MgO(3.0 nm) multilayers with respect to the nominal metallic layer thickness was investigated. A comparison with existing experimental data on discontinuous metal–insulator multilayers, ultrathin epitaxial Fe films on MgO substrates and granular cermet films is made. It is confirmed that the deposition conditions and the material composition play a crucial role in the percolation process. Nominal thicknesses of Fe layers at which an infinite metallic cluster is formed and the conditions for continuous Fe coverage were determined. Different methods of percolation threshold detection were analysed. We show that investigation of the temperature dependence of resistance in nanostructures could lead to an overestimation of the percolation threshold value, while magnetic measurements alone could lead to its underestimation.

1. Introduction

Physical properties of binary metal–insulator (cermet) mixtures have been studied both experimentally and theoretically for many years. The general approach to these studies involves effective media and percolation theories [1–4]. Percolation theory is applied if the conductivity of the metal phase (σ_m) is much higher than the conductivity of the insulator (σ_i). Usually a model binary mixture is characterized by the volume fraction of the metallic phase (x), the volume fraction of the insulator ($1 - x$) and the critical metal volume fraction (x_c). The latter corresponds to the composition at which the infinite metal cluster is first formed and conductivity starts to rise sharply. The dependence of the electrical conductivity of a cermet composite (σ_f) for $x > x_c$ could be described [1, 3] using the expression $\sigma_f = \sigma_m(x - x_c)^\alpha$, where α is a percolation exponent. Such a model faces serious difficulties for metallic binary composites in which both components have conductance of the same order of magnitude. In this case effective media theories and their modifications should be used [4–6]. It was believed [1, 5, 7, 8] that the percolation parameters x_c and α, whether determined by computer simulation using the lattice percolation model or experimentally in continuum composite, were universal, and that they depended only on the dimensions of the system. Recent studies of percolation processes in nanostructures and continuous systems show nonuniversality of these parameters [4, 9–11] and that the continuous percolation problem is fundamentally different from the lattice one [12, 13]. In cermet systems considerable values of conductance are observed in the so-called 'dielectric' regime [3, 9, 11, 14]. This is considered as a paradox because, in contradiction to classic percolation theory, the particles are not in direct electrical contact (as in the 'metallic' regime [3]) but any two particles are connected via tunnelling; i.e. the system is globally electrically connected for any concentrations of conductive particles [14–16]. Thus

the meaning of the percolation threshold and the origin of percolation behaviour have been under discussion. It was proposed to distinguish two different types of percolation scenarios depending on particle densities: one of tunnelling type and another caused by coalescence (direct contact) [16].

It was also shown experimentally that the concentration of metallic particles at which a continuous cluster is formed could vary in a wide range even for cermet films deposited in identical conditions with the same insulator (ZrO_2) but different metal phase (Ag, Co, Au) [17]. Besides, varying deposition conditions (i.e. temperature of the substrate) could cause a transition from two-dimensional (2D) continuous towards discontinuous three-dimensional (3D) film growth [18], resulting in different physical properties and microstructural characteristics. Thus, each particular percolation structure should be treated independently. There has been a wealth of literature regarding different scaling behaviours that are caused by the dimensionality of the percolation network [19, 20], irregularity in shapes and sizes of the particles [4, 5, 11, 21] and σ_i/σ_m value [4, 5] in cermet films and bulk composites.

From this point of view, the discontinuous metal–insulator multilayers (DMIM) [22, 23] are unique nanostructures that feature a transition from the 2D to 3D case. Unlike the convenient cermet films, the metallic nanoparticles in DMIM are situated not randomly within the film volume but regularly in layers that are separated from each other by a relatively thick insulator. This makes the percolation process within a single metallic layer close to the 2D case. On the other hand, in a stack of metal–insulator bilayers, equidistance between metallic granules along all spatial directions could be found for certain layer thicknesses and growth conditions [24]. Such a percolation system should be treated as 3D. Contrary to granular cermet films, DMIM are not usually characterized by a volume fraction of the metallic phase but by a nominal thickness of the metallic layer (t). Although the volume fraction could be derived from the relation between the thicknesses of the metal and insulator layers, the total thickness of DMIM varies with t, causing the change in dimensionality of the sample. Also, it is not quite clear how many metallic layers are involved in conductance. It is known [25] that a combination of current-in-plane (CIP) and current-perpendicular-to-plane (CPP) transport regimes could be distinguished even for CIP geometry of measurements. Thus, current could flow only within the first layer, uniformly within the whole sample with the same density in all planes or in various layers but with unequal densities. The estimation of the shape of current lines in DMIM as well as pinhole density is not an easy task. This makes the investigation of the percolation problem using the σ_f versus x (or t) dependence in DMIM puzzling. Consequently, one should use alternative methods to determine the percolation threshold in such structures. Among them the temperature dependence of resistance [26–30], magnetotransport and magnetic measurements [23, 24, 31, 32] and transmission electron microscopy (TEM) studies [17, 21, 22, 27, 29, 32] should be mentioned. The latter method proves to be very efficient for monolayers of Fe nanoparticles [29] and thin cermet films [17]. For DMIM, however, the structural state of the metallic layers for low and intermediate thickness is not always easily treated due to the superposition of the granules in different layers over the specimen thickness [24, 33]. Insulator–metal–insulator trilayers on grids for plane view TEM investigations could grow in different conditions and feature altered structural properties. Thus, magnetic and transport properties become of great importance for the determination of the percolation threshold in DMIM. In this paper we report the detection of the percolation threshold in Fe/MgO granular multilayers. Following different methods, our results are compared with the existing data on DMIM [22–24, 31, 34], MgO/Fe/MgO continuous and discontinuous trilayers [29], epitaxial Fe films on MgO substrates [35–44] and cermet granular films of different compositions [26–28, 30, 32, 45–47].

2. Experiment

Granular multilayers MgO(3 nm)/[Fe(t nm)/MgO(3nm)]$_N$ (0.4 nm $< t <$ 1.5 nm) were deposited on glass substrates by pulsed laser deposition (PLD). Here N is the number of bilayers in a stack. The details of film preparation, structural and magnetic characterization are reported elsewhere [33]. Electrical resistance and magnetoresistance (MR) measurements in the temperature range 10–300 K and in magnetic fields (H) up to 18 kOe were carried out using the four-point method (Keithley 236 current source and Agilent 34401 digital voltmeter) in an Oxford Spectrostat NMR He cryostat equipped with an ITC503 controller. A computer via Labview software managed the set-up. Two different orientations of magnetic field with respect to current-in-plane (I) were studied: (1) H in the film plane and parallel to I (L—longitudinal geometry) and (2) H in the film plane but perpendicular to I (T—transverse geometry). The values of MR were determined using the formula MR $= [\rho(H) - \rho(0)]/\rho(0)$, where $\rho(0)$ and $\rho(H)$ are the resistivity of the film in zero field and in an applied magnetic field H, respectively.

Magnetic measurements were performed in a Quantum Design MPMS 5S superconducting quantum interference device magnetometer in the 5–300 K temperature range with magnetic field applied in the film plane.

3. Results and discussion

First we shall analyse the mechanisms of conductance in the films. Temperature dependences of ρ for the films with $t = 0.53$ and 0.61 nm are shown in figure 1. Experimental data could be fitted using the expression for low electric field limit tunnelling conductance [26, 27] $\rho \sim \exp(2\sqrt{C/k_BT})$, where k_B is the Boltzmann constant and C the tunnelling constant related to average interparticle distance and charging energy necessary to generate a pair of charged granules. The values of C decrease with increasing t from 270 meV ($t =$ 0.53 nm) to 34 meV ($t = 0.61$ nm). This variation reflects an increase in particle size and a reduction in distances between them [26–28, 30, 46]. The decrease of tunnelling constant with

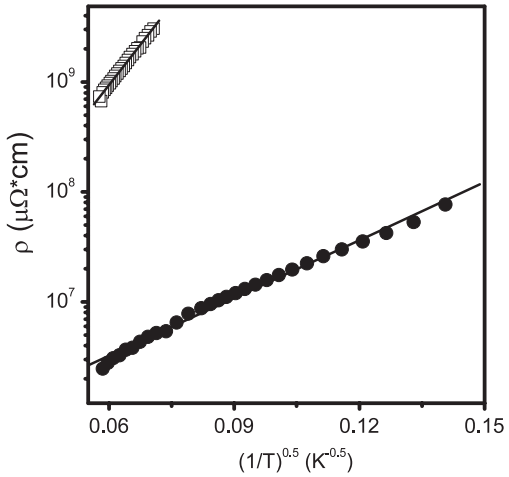

Figure 1. Temperature dependences of resistivity (ρ) for Fe(t nm)/MgO(3 nm) layered granular films: $t = 0.53$ nm (open squares), $t = 0.61$ nm (solid circles). Solid lines represent a fit of the experimental data using a $\rho \sim \exp(2\sqrt{C/k_BT})$ dependence.

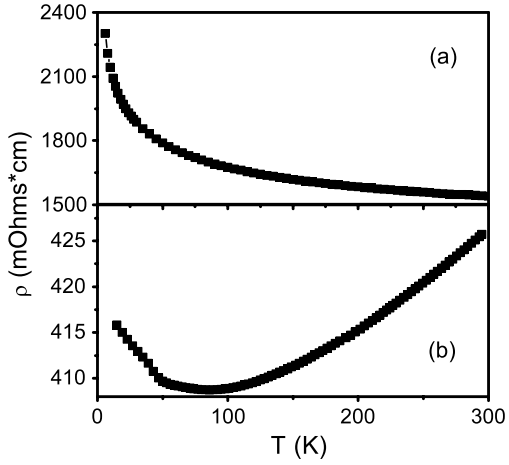

Figure 2. Temperature dependences of resistivity (ρ) for Fe(t nm)/MgO(3 nm) layered granular films: $t = 0.81$ nm (a) and $t = 1.25$ nm (b).

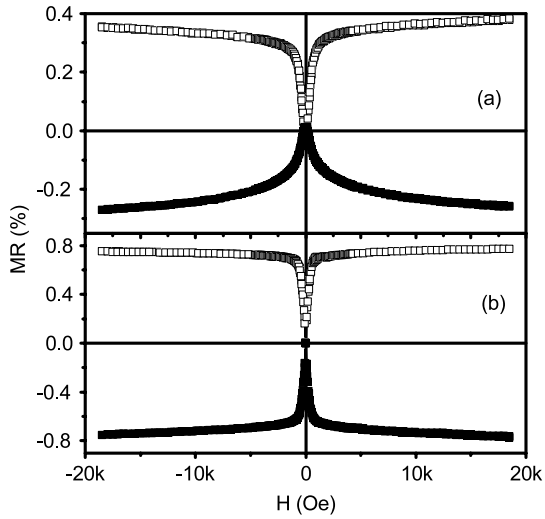

Figure 3. Dependences of magnetoresistance (MR) versus the applied magnetic field (H) for Fe(t nm)/MgO(3 nm) layered granular films: $t = 0.81$ nm (a) and $t = 1.25$ nm (b). Measurements in L-geometry (open symbols) and T-geometry (closed symbols) at $T = 300$ K.

increasing t in our case in general corresponds to that reported for granular cermets. For example, in [28] C decreases from ∼250 to ∼50 meV as the volume fraction of the metallic phase in the Co-SiO_2 composite increases from $x \sim 0.1$ to ∼0.3. A rapid decrease of C in our case reflects differences in film structure and composition.

Previous magnetic and TEM studies [33] show that Fe layers in the films with $t \leqslant 0.61$ nm are discontinuous. Magnetically the films could be described as an ensemble of noninteracting superparamagnetic particles. Magnetotransport measurements confirm the granular nature of Fe layers. Resistance of the film with $t \leqslant 0.61$ nm decreases continuously with increasing H. Magnetoresistance measured in L- and T-geometries coincides, indicating a typical behaviour of tunnelling MR for granular cermet films in the dielectric regime [27, 33, 46].

The dependences $\rho(T)$ and MR(H) for samples with $t \geqslant 0.81$ nm are shown in figures 2 and 3, respectively. Predominantly metallic conductance and anisotropic magnetoresistance (AMR) for $t = 1.25$ nm clearly hint that the film contains a continuous metallic ferromagnetic layer. However, the value of ρ is high, compared to bulk Fe, and the dependence $\rho(T)$ is relatively weak and nonmonotonic. A shallow minimum is observed at $T \approx 100$ K. Such behaviour seems to be a characteristic feature of ultrathin and disordered metallic films [35, 37, 48–50]. It can be explained in terms of electron localization and/or electron–electron interaction effects [35, 37, 51]. The position of the minimum is shifted towards higher temperatures compared to epitaxial Fe films of $t = 1.8$ nm deposited on MgO(001) substrates [37]. This is caused by the stronger influence of localization processes, and surface and defect scattering associated with reduced Fe layer thickness and a higher degree of structural disorder in our case.

We should point out that the value of AMR ∼ 0.8% obtained in the sample with $t = 1.25$ nm is much higher than that of bulk Fe (0.15%) for the same magnetic field [52]. An enhanced value of the AMR (up to 1%) in ultrathin epitaxial Fe films sandwiched between MgO layers has also been found in [44] and ascribed to 2D confinement effects which result from quantum interference within the heterostructure and distorted Fe band structure.

The film with $t = 0.81$ nm shows mixed properties. The dependence $\rho(T)$ has activation characteristics (figure 2(a)). The resistance of the films continuously drops with increasing temperature. However, the fit using the $\rho \sim \exp(2\sqrt{C/k_BT})$ law gives an unrealistically small ($C < 0.1$ meV) activation energy. At the same time the AMR effect typical for continuous ferromagnetic films is found (figure 3(a)). The value of AMR for the sample $t = 0.81$ nm is still higher than for bulk Fe, however, it is reduced by a factor ∼2 compared to the sample $t = 1.25$ nm. One can mentioned slight asymmetry in AMR behaviour for the film $t = 0.81$ nm. It could be caused either

by a slight misalignment of the sample with respect to the magnetic field or a change of the samples resistance during measurement due to a small temperature drift. The difference in AMR for positive and negative field is less than ±3%, which corresponds to experimental error.

Qualitatively similar $\rho(T)$ behaviour was observed [31] for a film of composition $[Co_{80}Fe_{20}(1.7\ nm)/Al_2O_3(3\ nm)]_{10}$. It was suggested that this sample is just below the global (geometrical) percolation of the metallic phase. It contains big fractal clusters separated with thin tunnel barriers. As a result the characteristics of the $\rho(T)$ dependence are determined by the competition of the electron transport within the clusters and the tunnelling between them. Magnetic data on that film shows the formation of a superferromagnetic (SFM) state while the AMR effect was small and covered with strong noise. Unfortunately in [30] the dependences $\rho(T)$ and AMR were presented in arbitrary units and we are not able to compare data quantitatively. Contrary to the data on $[Co_{80}Fe_{20}(1.7\ nm)/Al_2O_3(3\ nm)]_{10}$ DMIM, our MR measurements did not reveal strong noise. Also magnetic properties of our sample with $t = 0.81$ nm are different and the magnetic state of the film is close to the bulk ferromagnet [33], i.e. the hysteresis loops are easily saturated in relatively low fields and demonstrate a weak temperature dependence of magnetization. This allows the presumption that a continuous Fe cluster is present in the film.

Submillivolts activation energy $\rho(T)$ behaviour was observed earlier [35] for epitaxial Fe film with $t = 0.8$ nm on a MgO substrate. It was explained within a frame of conductance in disordered 2D metals involving weak localization and interaction effects. Also, a crossover from the 2D disordered conductor to the 3D metallic regime was found in the range $0.8\ nm < t < 1.2\ nm$. Although our films are not epitaxial, the characteristics of $\rho(T)$ behaviour observed in this work correspond very well with those reported in [35].

The dependence of resistivity ρ versus t at $T = 295$ K is shown in figure 4. Experimental data of this work are compared with the data on discontinuous MgO/Fe/MgO trilayers [29] and thin epitaxial Fe films on MgO substrates [35–37]. It is clearly seen that our data in the $t > 0.81$ nm limit correspond pretty well with those of continuous Fe films. Taking into account that ρ values were recalculated using the total thickness of all Fe layers we can conclude that the current is flowing uniformly within all layers [25] and continuous Fe layers have a well ordered crystalline structure. With decreasing t below 0.81 nm a sharp increase of ρ occurs. Such an increase was found in [29] for MgO(2.0 nm)/Fe(t nm)/MgO(2.0 nm) trilayers for $t < 1.0$ nm and was attributed to the transition of the Fe layer structure from a continuous film to a discontinuous one. Our magnetic, TEM and $\rho(T)$ data confirm the appearance of discontinuous Fe layers for similar values of t.

The solid line in figure 4 represents model percolation behaviour calculated with universal parameters $x_c = 0.16$ and $\alpha = 1.9$. However, the meaning of these parameters and the applicability of the phenomenological percolation approach must be justified. It was shown earlier that the experimentally determined value of x_c is the percolation threshold of an

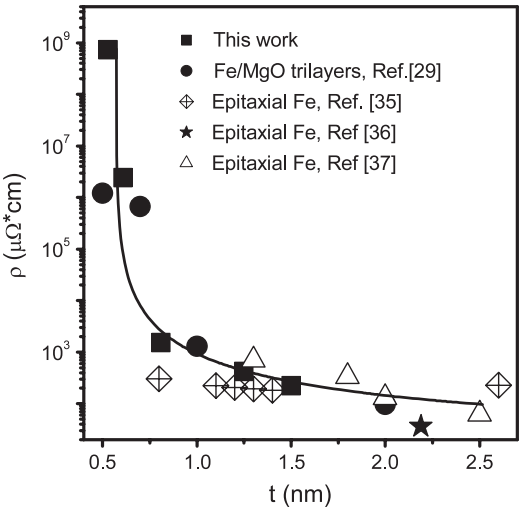

Figure 4. Dependence of electrical resistivity (ρ) versus Fe layer thickness (t) for Fe(t nm)/MgO(3 nm) layered granular films. Measurements were carried out at $T = 295$ K. Our data are compared with those of [29, 35–37]. The solid line represents the best fit using the percolation model $\sigma_f \sim (x - x_c)^\alpha$ with $x_c = 0.16$ and $\alpha = 1.9$. Metallic volume fraction (x) was recalculated as a relation of Fe layer thickness (t) to total thickness of Fe/MgO bilayer.

electrical network in which only the tunnelling of nearest neighbours contributes to the conduction [14]. This is the only case where the system behaves as a genuine percolation one. The percolation parameters determined in nanostructures with dominant tunnelling conductance, even if they are close to universal, have very little to do with the criteria established for the systems of hard spheres [53] but rather reflect specific structural and transport properties [54]. Recently, the model of tunnelling percolation has been developed further [15]. A 3D system of spherical conductive particles with average diameter d randomly situated in a dielectric matrix is used as a starting point for modelling. Around each particle a soft shell of constant thickness ξ is introduced. It is suggested that two conductive particles become electrically connected when their soft shells overlap, i.e. the separation between their closest surfaces is less than a certain upper cut-off limit ξ_c. In a cermet system containing metal nanoparticles dispersed in an insulator host, the shell thickness can be physically interpreted as a characteristic tunnelling length, governing the electrical connectivity of the composite. The value of ξ_c in real systems is usually set to ∼1 nm [9]. The model predicts nonuniversal values for the percolation exponent α and the dependence of x_c on ξ_c/d. The electrical connectivity of the system is established for concentration values that are rapidly decreasing as ξ_c/d increases. This result is of great importance for nanogranular structures where the sizes of metallic granules are comparable to the characteristic tunnelling length, i.e. a percolation conductive network could be formed at a very low concentration of metallic material.

However, direct application of this model faces certain difficulties in our case. The films under investigation do not satisfy the criterion of a convenient 3D system used in modelling. Metallic particles are situated in layers well

separated from each other by a relatively thick 3 nm MgO barrier. This system is highly anisotropic. The distances between Fe particles within the same layer decrease with increasing t, while the distances between adjacent layers remain almost the same. This means that tunnelling between particles within a layer will have higher probability (especially for t values close to geometrical percolation of metallic particles) compared to interlayer tunnelling. This can explain why the experimental points in figure 4 correlate with the percolation curve calculated for relatively low x_c.

Another aspect that is widely missed in percolation models requires modification associated with the magnetic nature of the metallic material. It is well known [55, 56] that tunnelling probability in ferromagnetic nanostructures depends on the relative magnetization of neighbour granules, i.e. it is higher when magnetic moments of the granules are oriented ferromagnetically and lower for antiferromagnetic orientation. It terms of the model proposed in [15], this means that ξ_c should be dependent on the direction of the granules' magnetization. It is not clear whether introduction of a broad distribution of 'cut-off' distances will model this behaviour. To our best knowledge no percolation model that accounts for the effects of spin-dependent transport on the tunnelling percolation process has yet been developed.

It has to be pointed out that the tunnelling percolation mechanism is different from the one associated with direct electrical (geometrical) contact of conductive particles (for example, due to the coalescence process in granular cermets [27]). This explains the discrepancy in percolation threshold determination using ρ versus x and ρ versus T dependences. Usually analysis of the temperature coefficient of resistance (TCR) would lead to overestimation of the percolation threshold value. Activation characteristics of $\rho(T)$ could be caused not only by tunnelling conductance but also by a strong contribution from surface and defect scattering, electron localization and electron–electron interaction effects [35, 51, 57, 58]. Mooij [48] predicts negative TCR for continuous transition-metal thin films with $\rho > 150$ $\mu\Omega$ cm due to strong scattering and reduced electron mean free path. However, our film with $t = 0.81$ nm shows the value of resistance ~1500 $\mu\Omega$ cm at room temperature (RT) that is one order of magnitude higher. On the other hand, activation characteristics of $\rho(T)$ above the percolation threshold were reported earlier for a number of granular cermets. For example, the percolation threshold for electron beam deposited Co_x–$(Al_2O_3)_{1-x}$ films was determined from the ρ versus x curve [45] to be $x \approx 0.25$, while TCR at RT becomes positive only at $x \sim 0.7$. For $(Co_{50}Fe_{50})_x$–$(Al_2O_3)_{1-x}$ prepared by electron beam deposition [46] these values were ≈0.17 and ≈0.35, respectively, and metallic conductance in a wide temperature range was observed for $x > 0.45$. The temperature dependence of resistance of granular cermets Pt_x–$(Al_2O_3)_{1-x}$ was studied in [47]. It was found that samples with $x \geqslant 0.59$ behave like dirty metals. Their resistivities decrease with decreasing temperature until impurity scattering dominates and $\rho(T)$ becomes temperature independent. The resistive transition from predominantly metallic conduction to predominantly thermally assisted tunnelling occurs in the range of $0.50 < x < 0.59$. The general property of all those cases as well as in those reported in [26–28] is that the TCR at RT changes sign in the range $\rho \sim 10^3 \mu\Omega$ cm that corresponds to the Mott limit for the minimum conduction in disordered metallic materials [51, 59]. The value of resistivity of our sample with $t = 0.81$ nm is within this range and scattering conditions for non-metallic conductance could appear, i.e. the criterion TCR > 0 in nanostructured cermets reflects the formation of a continuous, well ordered metallic film (geometrical percolation) rather than establishing a tunnelling percolation network.

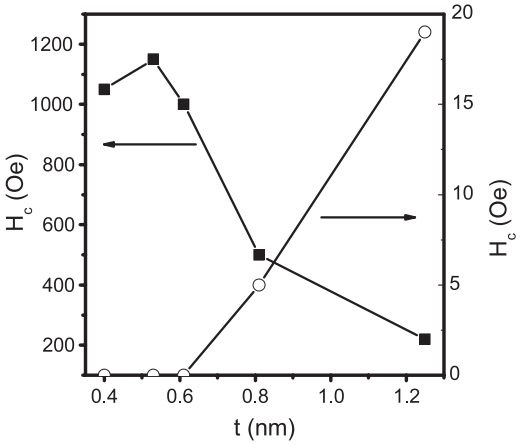

Figure 5. The dependence of coercive field (H_c) versus Fe layer nominal thickness (t) at $T = 5$ K (solid squares) and $T = 295$ K (open circles).

An alternative way to detect the percolation threshold in magnetic granular nanostructures involves analysis of the dependence of coercive field (H_c) versus t [32]. Our results measured at $T = 5$ and 300 K are presented in figure 5. At $T = 5$ K H_c first increases with t reaching the value of ~1200 Oe at $t = 0.53$ nm and then drops down to ~200 Oe for $t = 1.25$ nm. The latter value of H_c is much higher than that of bulk Fe. This effect is caused by strong surface anisotropy due to the formation of an FeO_x oxide layer on the Fe/MgO interface [18, 33, 60]. The shape of the H_c versus t curve at $T = 5$ K is similar to the one reported for Fe–SiO_2 granular films [32]. The decrease of H_c with a further increase of Fe content was attributed to a percolation effect. As the volume fraction of Fe approaches the percolation threshold, conglomerates of small granules start to form. Due to dipolar interaction, magnetic closure-domain structure would be preferable and the system behaves as a multidomain. As a result coercivity decreases. Thus the maximum of H_c could be considered as a signature of approaching the percolation threshold.

A similar shape of $H_c(x)$ behaviour was held for granular cermets in the whole range of temperatures [32] and $H_c \sim 500$ Oe was reported for $T = 300$ K. In our case the dependence $H_c(t)$ for $T = 295$ K is qualitatively different from that of granular films. No irreversible behaviour was found in our samples [33] for $t < 0.81$ nm. For higher thicknesses a narrow hysteresis loop was observed. This

behaviour is similar to the one studied by the magneto-optical Kerr effect for DMIM [23, 31] in which continuous 2D ferromagnetic layers are formed. However, in that case an offset of ferromagnetism appears well below the geometrical percolation threshold caused by coalescence of the metallic phase. It was suggested [24, 31] that dipolar stray fields between finite-size granules (superspins) can produce ferromagnetic coupling and that this 'superexchange' can give rise to SFM order in 2D granular systems above some critical value of diameter-to-interparticle distance ratio. It is possible to assume that the case of SFM order could be treated using a similar 'hard core–soft shell' model proposed for tunnelling conductance [15]. In this case the thickness of the soft shell should represent the characteristic dipole interactions' cut-off length. At this point it is not clear whether the dipole 'cut-off' distance should be taken as higher or lower than the tunnelling one.

Besides, one should keep in mind that the presence of the oxide layer on the surface of nanoparticles together with spin surface disorder [61] could be the reason for the extremely high coercive field values especially at low temperatures. As a result, magnetization measurements alone provide valuable information that, however, could lead to an underestimation of the threshold value as irreversible behaviour caused by dipole or exchange interactions could be misinterpreted as the formation of a continuous percolation cluster.

We would like also to emphasize the influence of deposition techniques and material composition. Our data show certain similarities to DMIM of composition $Co_{80}Fe_{20}(t\ \text{nm})/Al_2O_3(3\ \text{nm})$ reported in [23, 31]. However, in that case metallic conductance is observed and continuous CoFe layers are formed at $t = 1.8$ nm. Percolation of the metallic layer was also found [22] for Co/SiO_2 DMIM at $t = 2.0$ nm. The nominal thickness of Fe layers at which metallic conductance appears and a continuous Fe cluster is formed are lower in our case. This could be caused by different nucleation and growth conditions in the Fe/MgO system. It is well known that deposition of Fe on single-crystal MgO at RT gives rise to 2D epitaxial growth [43]. Complete coverage of the MgO substrate by ultrathin sputtered Fe films was found around six monolayers (ML). Taking into account that 1 ML thickness [40] is ∼0.143 nm one could expect for certain deposition conditions [43] continuous Fe film at $t \sim 0.9$ nm. This is quite different from the $Co_{80}Fe_{20}(t\ \text{nm})/Al_2O_3(3\ \text{nm})$ system for which equal distance between metallic granules in all spatial directions was predicted [24] for $t = 0.9$ nm. However, one should keep in mind that Fe growth on MgO is deposition condition sensitive and controversial results have been reported for this system. For example, the percolation threshold was detected by means of infrared transmission spectroscopy at $t \leqslant 0.7$ nm for electron beam evaporated Fe film deposited on MgO(001) air-cleaved surfaces and at $t \leqslant 1.0$ nm for ultra-high vacuum cleaved surfaces [38]. Bulk-like Fe films of 5 ML thickness were deposited [39] by electron beam evaporation at RT. Electron beam evaporated Fe films of thickness up to 10 ML grown at 700 K were found to be superparamagnetic but show ferromagnetic behaviour if deposited at RT [40]. The influence of miscut angle of single-crystal MgO substrates in the magnetic percolation of epitaxial Fe films has been pointed out [43], as even for perfect 2D growth the maximum lateral size of Fe domains in a 1 ML film would be that of the substrate terraces. Also it was found that a percolation cluster is formed before complete coverage of the surface takes place [62]. Generally [35, 40–42], the formation of continuous Fe films is reported for 10 ML thickness, which corresponds to $t \sim 1.43$ nm.

Very similar results were also reported [34] for Fe/ZrO_2 multilayers prepared by magnetron sputtering. Continuous Fe layers were formed for $t > 1.2$ nm. At the same time extended x-ray absorption fine structure (EXAFS) and Mössbauer spectroscopy confirm the development of amorphous or ill-ordered continuous metallic layers with Fe–Fe bond lengths slightly larger than in BCC iron at t as low as 0.6 nm. These layers coexist with superparamagnetic Fe particles of a few nm size and high-spin non-magnetic Fe^{2+} and Fe^{3+} ions. The structure of the films with $0.6\ \text{nm} < t < 0.9$ nm was described as: magnetic metal/not well defined ionic compound/oxide. The relative amount of intermixed region decreases with t, and a multilayer with $t = 1.5$ nm was considered as one with continuous metallic layers that has lost one monoatomic iron layer by oxidation at each interface. Our films with $t < 0.61$ nm represent an ensemble of superparamagnetic particles with Fe core/FeO_x shell structure [32] similar to that reported in [34]. However, we do not detect any ferromagnetic contribution in the range of $t < 0.61$ nm. The formation of continuous Fe layers and the onset of ferromagnetism in our case take place at $t \sim 0.8$ nm.

The deposition conditions in our case are different from those of [34–44] and we should not expect that the structural, magnetic and transport properties of our films would show one-to-one correspondence to those reported earlier. Judging our magnetic and magnetotransport data, the sample with $t = 1.25$ nm contains almost continuous though disordered Fe layers. The structural state of Fe layers in the sample with $t = 0.81$ nm (∼5.4 ML of Fe) could be described as a 2D dendritic containing backbone with bottlenecks surrounded by dead branches, i.e. Fe layers are percolated but conditions of continuous coverage are not fulfilled. This structure together with atomic disorder and surface oxidation cause a reduction of AMR values and give rise to the activation mechanisms of conductance observed in experiment.

4. Conclusions

Magnetic and transport measurements were used to study the percolation process and formation of continuous metallic layers in a series of granular Fe/MgO multilayers. Our investigations confirm that in nanostructures in which tunnelling is the dominant mechanism of conductance the criterion $\text{TCR} > 0$ detached could mislead to percolation threshold overestimation as it points not to the formation of a percolation network but rather to the presence of a continuous well ordered metallic layer. A negative temperature coefficient of resistance could be found both for a system of nanoparticles connected by tunnelling and in ill-ordered ultrathin metallic films. Magnetometry used alone could lead to an underestimation of the percolation threshold value due to

the onset of cooperative behaviour of magnetic nanoparticles caused by dipolar interactions. It was shown that, for the investigated Fe/MgO structures, metallic particles form geometrically percolated layers at nominal Fe thickness $t = 0.81$ nm. This is reflected both by the rapid decrease in the film resistance and the onset of ferromagnetic properties. Thickness and temperature dependences of conductance for $t > 0.81$ nm give an example of a crossover from disordered 2D to a 3D metallic regime observed earlier for epitaxial Fe films. Our data were compared with those published previously for MgO/Fe/MgO granular trilayers and epitaxial films, demonstrating good correlation and confirming the general tendency of iron growth on the MgO substrate or buffer layer. The obtained value of the nominal thickness at which the infinite metallic percolation cluster is formed is lower than for CoFe (Co) layers on Al_2O_3 (SiO_2) oxides, indicating differences in nucleation and growth of the metal layer. This supports the statement that percolation processes in nanostructures must be considered individually, depending on the given material composition and growth procedure.

Acknowledgments

Financial support by the Spanish Ministry of Science (through project MAT2008-06567-C02 and CIT-420000-2008-19 including FEDER funding) and by the Aragon Regional Government (through projects E26 and PI059/08) is acknowledged.

References

[1] Kirkpatrick S 1973 *Rev. Mod. Phys.* **45** 574
[2] Kirkpatrick S 1971 *Phys. Rev. Lett.* **27** 1722
[3] Abeles B, Pinch H L and Gittleman J I 1975 *Phys. Rev. Lett.* **35** 247
[4] Wu J and McLachlan D S 1997 *Phys. Rev.* B **56** 1236
[5] McLachlan D S, Blaszkiewicz M and Newnham R E 1990 *J. Am. Ceram. Soc.* **73** 2187
[6] McLachlan D S 1997 *J. Phys. C: Solid State Phys.* **20** 865
[7] Stauffer D 1979 *Phys. Rep.* **54** 1
[8] Lee S I, Song Y, Noh T W, Chen X D and Gaines J R 1986 *Phys. Rev.* B **34** 6719
[9] Balberg I 1987 *Phys. Rev. Lett.* **59** 1305
[10] Kogut P M and Starley J P 1979 *J. Phys. C: Solid State Phys.* **12** 2151
[11] Kusy R P 1977 *J. Appl. Phys.* **48** 5301
[12] Watson B P and Leath P L 1974 *Phys. Rev.* B **9** 4893
[13] Garfunkel G A and Weissman W B 1985 *Phys. Rev. Lett.* **55** 296
[14] Toker D, Azulay D, Shimoni N, Balberg I and Millo O 2003 *Phys. Rev.* B **68** 041403
[15] Johner N, Grimaldi C, Balberg I and Ryser P 2008 *Phys. Rev.* B **77** 174204
[16] Balberg I 2009 *J. Phys. D: Appl. Phys.* **42** 064003
[17] García Del Muro M, Konstantinovic Z, Varela M, Batlle X and Labarta A 2008 *J. Nanomater.* **2008** 475168
[18] Cebollada F, Hernando-Mañeru A, Hernando A, Martínez-Boubeta C, Cebollada A and González J M 2002 *Phys. Rev.* B **66** 174410
[19] Clerc J P, Giraud G, Alexander S and Guyon E 1980 *Phys. Rev.* B **22** 2489
[20] Rappaport M L and Entin-Wohlman O 1983 *Phys. Rev.* B **27** 6152
[21] Kim W J, Taya M, Yamada K and Kamiya N 1998 *J. Appl. Phys.* **83** 2593
[22] Dieny B, Sankar S, McCartney M R, Smith D J, Bayle-Guillemaud P and Berkowitz A E 1998 *J. Magn. Magn. Mater.* **185** 283
[23] Kakazei G N, Pogorelov Yu G, Lopes A M L, Sousa J B, Cardoso S, Freitas P P, Pereira de Azevedo M M and Snoeck E 2001 *J. Appl. Phys.* **90** 4044
[24] Kleemann W, Petracic O, Binek Ch, Kakazei G N, Pogorelov Yu G, Sousa J B, Cardoso S and Freitas P P 2001 *Phys. Rev.* B **63** 134423
[25] Ernult F, Giacomoni L, Marty A, Dieny B, Vedyayev A and Ryzhanova N 2002 *Eur. Phys. J.* **25** 177
[26] Gittleman J L, Golstein Y and Bozowsky S 1972 *Phys. Rev.* B **5** 3609
[27] Abeles B, Sheng P, Coutts M D and Arie Y 1975 *Adv. Phys.* **24** 401
[28] Barzilai S, Goldstein Y, Balberg I and Helman J S 1981 *Phys. Rev.* B **23** 1809
[29] Arita M, Wakasugi K, Ohta K, Hamada K, Takahashi Y and Choi J B 2008 *Microelectron. Eng.* **85** 2445
[30] Hattink B J, García Del Muro M, Konstantinovic Z, Puntes V F, Batlle X, Labarta A and Varela M 2005 *Int. J. Nanotechnol.* **2** 43
[31] Sousa J B, Santos J A M, Silva R F A, Teixeira J M, Ventura J, Araujo J P, Freitas P P, Cardoso S, Pogorelov Yu G, Kakazei G N and Snoeck E 2004 *J. Appl. Phys.* **96** 3861
[32] Xiao G and Chien C L 1987 *Appl. Phys. Lett.* **51** 1280
[33] García-García A, Vovk A, Pardo J A, Štrichovanec P, Magén C, Snoeck E, Algarabel P A, De Teresa J M, Morellón L and Ibarra M R 2009 *J. Appl. Phys.* **105** 063909
[34] Auric P, Micha J S, Proux O, Giacomoni L and Regnard J R 2000 *J. Magn. Magn. Mater.* **217** 175
[35] Liu C, Park Y and Bader S D 1991 *J. Magn. Magn. Mater.* **111** L225
[36] Schad R, Belien P, Verbanck G, Moshchalkov V V and Bruynseraede Y 1998 *J. Phys.: Condens. Matter* **10** 6643
[37] Sangiao S, Morellon L, Simon G, De Teresa J M, Pardo J A, Arbiol J and Ibarra M R 2009 *Phys. Rev.* B **79** 014431
[38] Fahsold G, Priebe A, Magg N and Pucci A 2000 *Thin Solid Films* **364** 177
[39] Luches P, Torelli P, Benedetti S, Ferramola E, Gotter R and Valeri S 2007 *Surf. Sci.* **601** 3902
[40] Park Y, Adenwalla S, Felcher G P and Bader S D 1995 *Phys. Rev.* B **52** 12779
[41] di Bona A, Giovanardi C and Valeri S 2002 *Surf. Sci.* **498** 193
[42] Fahsold G, Pucci A and Rieder K-H 2000 *Phys. Rev.* B **61** 8475
[43] Martínez-Boubeta C, Clavero C, García-Martín J M, Armelles G, Cebollada A, Balcells Ll, Menéndez J L, Peiró F, Cornet A and Toney M F 2005 *Phys. Rev.* B **71** 014407
[44] Martínez-Boubeta C, Balcells Ll and Cebollada A 2006 *Appl. Phys. Lett.* **88** 132511
[45] Niklasson G A and Granqvist C G 1984 *J. Appl. Phys.* **55** 3382
[46] Vovk A, Wang J Q, He J, Zhou W, Pogoriliy A, Shypil' O, Kravets A and Khan H 2002 *J. Appl. Phys.* **91** 10017
[47] Mantese J V, Curtin V A and Webb W W 1986 *Phys. Rev.* B **33** 7897
[48] Mooij J H 1973 *Phys. Status Solidi* A **17** 521
[49] Vovk A, Malkinski L, Golub V, O'Connor C, Wang Zh and Tang J 2005 *J. Appl. Phys.* **97** 10C503
[50] Vovk A, Yu M, Malkinski L, O'Connor C, Wang Zh, Durant E, Tang J and Golub V 2006 *J. Appl. Phys.* **99** 08R503
[51] Lee P A and Ramakrishnan T V 1985 *Rev. Mod. Phys.* **57** 287
[52] Tondra M, Lottis D K, Riggs K T, Chen Y, Dahlberg E D and Prinz G A 1993 *J. Appl. Phys.* **73** 6393
[53] Scher H and Zallen R 1970 *J. Chem. Phys.* **53** 3759

[54] Balberg I and Binenbaum N 1987 *Phys. Rev.* B **35** 8749
[55] Slonczewski J C 1989 *Phys. Rev.* B **39** 6995
[56] Inoue J and Maekawa S 1996 *Phys. Rev.* B **53** R11927
[57] Fuchs K 1938 *Proc. Camb. Phil. Soc.* **34** 100
[58] Sondheimer E H 1952 *Adv. Phys.* **1** 1
[59] Mott N F and Davis E A 1979 *Electronic Process in Non-Crystalline Materials* (Oxford: Clarendon)
[60] Meyerheim H L, Popescu R, Kirschner J, Jedrecy N, Sauvage-Simkin M, Heinrich B and Pinchaux R 2001 *Phys. Rev. Lett.* **87** 076102
[61] Kodama R H, Berkowitz A E, McNiff E J Jr and Foner S 1996 *Phys. Rev. Lett.* **77** 394
[62] Elmers H J, Hauschild J, Höche H, Gradmann U, Bethge H, Heuer D and Köhler U 1994 *Phys. Rev. Lett.* **73** 898